

---Supporting Information---

Electrosynthesis of nitriles from primary alcohols and ammonia on Ni catalyst

Yiyi Xiao^{a, b}, Chia Wei Lim^b, Linfeng Gao^b, Ning Yan^{*, a, b}

^a *Joint School of National University of Singapore and Tianjin University, International Campus of Tianjin University, Binhai New City, Fuzhou 350207, China*

^b *Department of Chemical and Biomolecular Engineering, National University of Singapore, 4 Engineering Drive 4, Singapore 117585*

*Corresponding author:

Ning Yan

Email: ning.yan@nus.edu.sg

Postal address: Department of Chemical and Biomolecular Engineering, National University of Singapore, 4 Engineering Drive 4, Singapore 117585, Singapore.

Table of Contents

Number of pages in the supporting information: 45

Number of figures in the supporting information: 29

Number of tables in the supporting information: 6

Number of schemes in the supporting information: 3

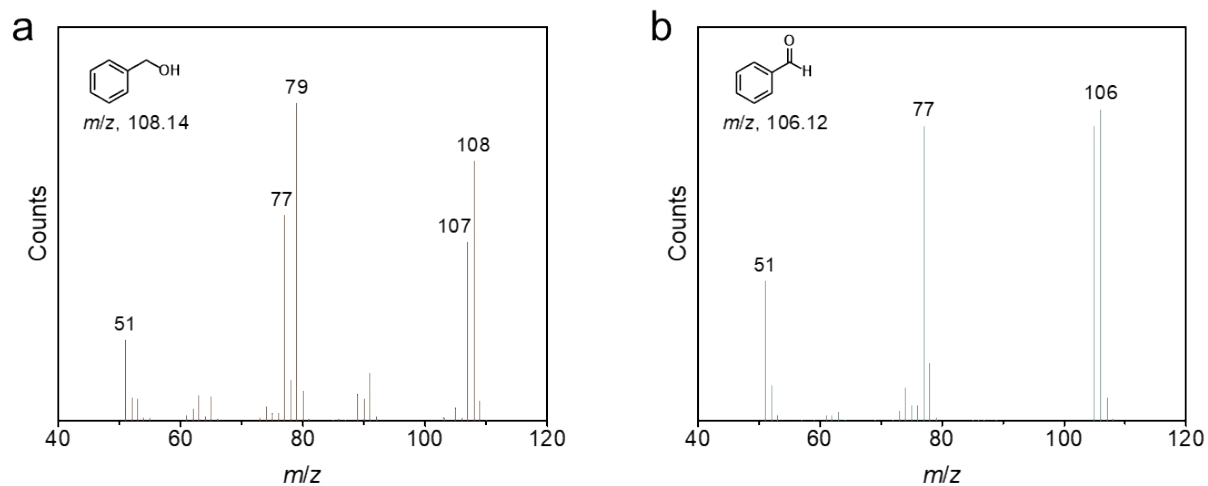


Figure S1 GC-MS analysis of the extracted liquid carbonaceous compounds obtained from the reaction. Corresponding MS spectra of **a)** benzyl alcohol and **b)** benzaldehyde. Reaction conditions: Ni foam, 20 mM BnOH, 1 M NH_3 , pH 13, 1.425 V vs. RHE, 12 h reaction time.

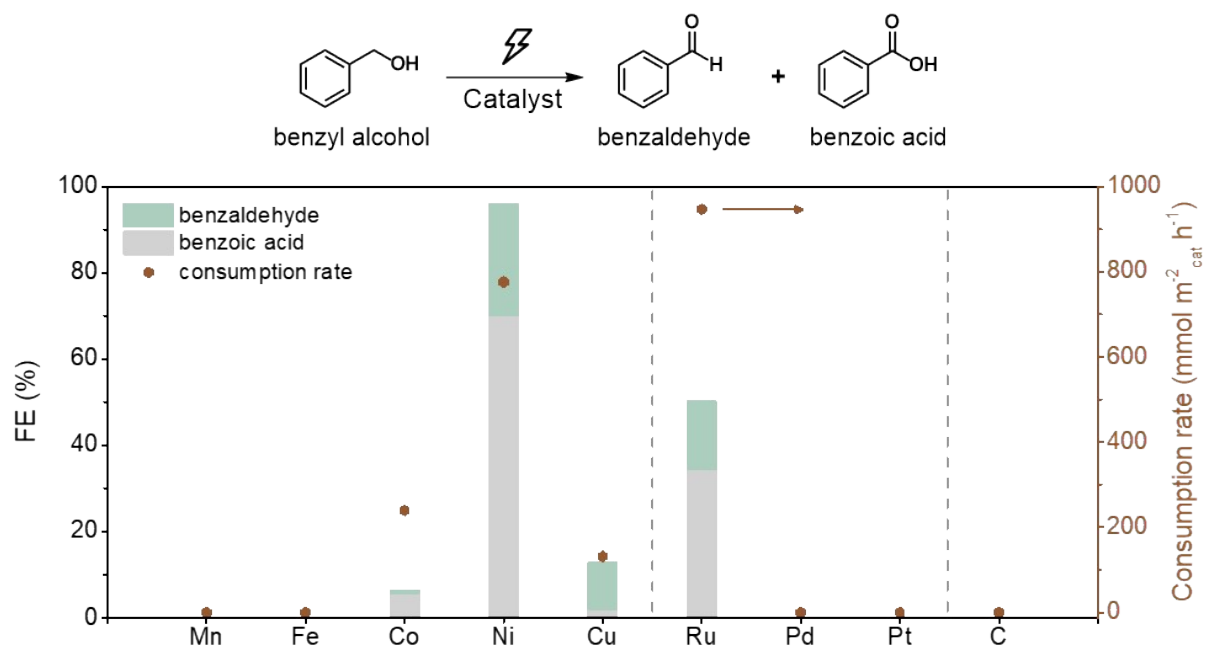
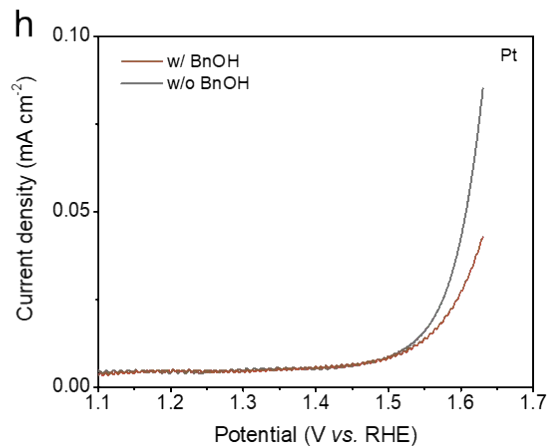
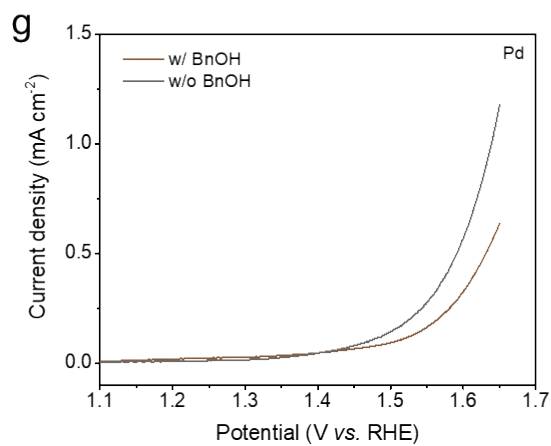
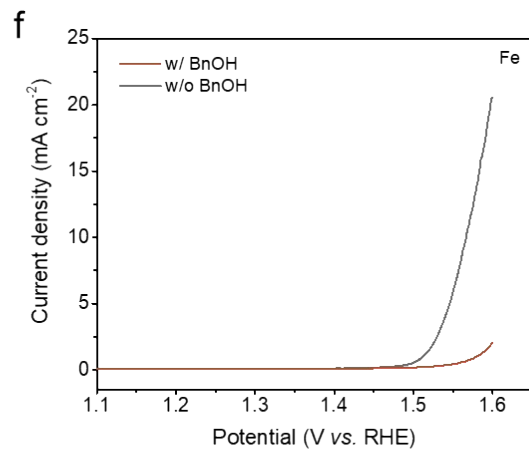
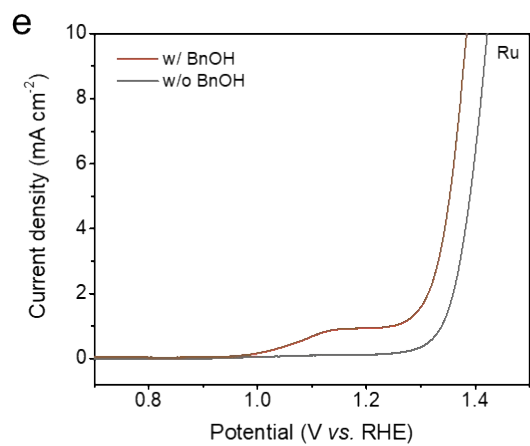
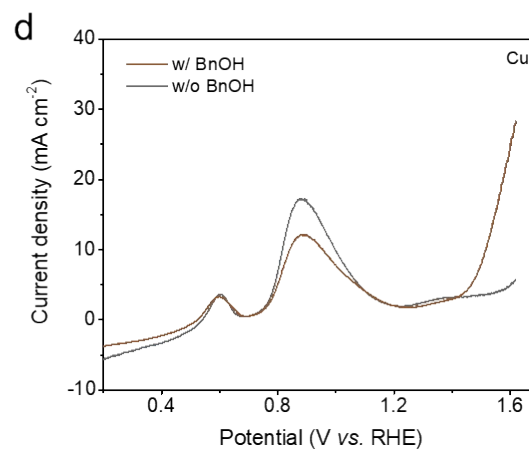
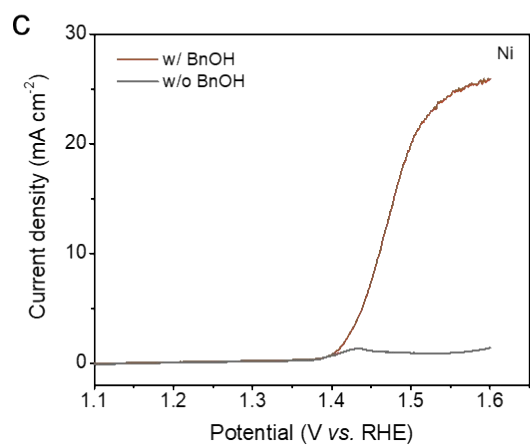
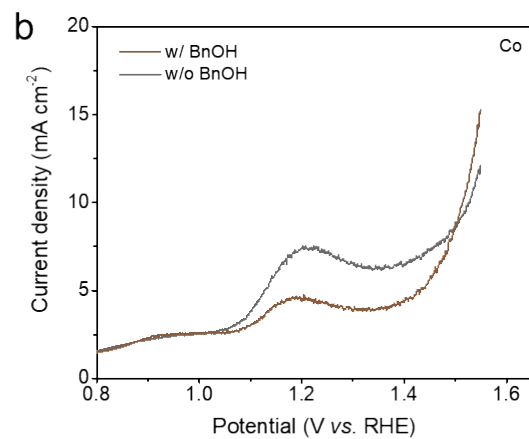
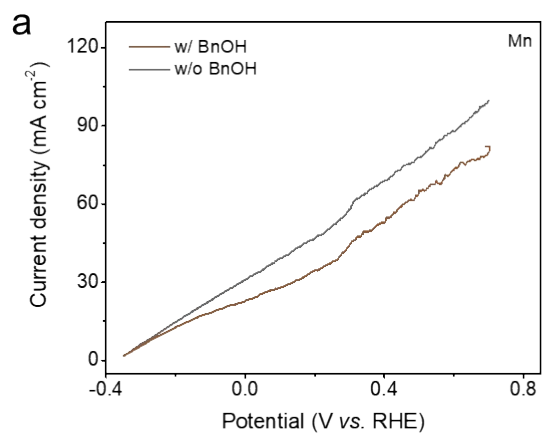


Figure S2 FEs and BnOH consumption rate of electro-oxidation of BnOH on various catalysts. Reaction conditions: 20 mM BnOH, pH 13, 1.425 V vs. RHE (-0.265 V vs. RHE for Mn), 1 h reaction time.



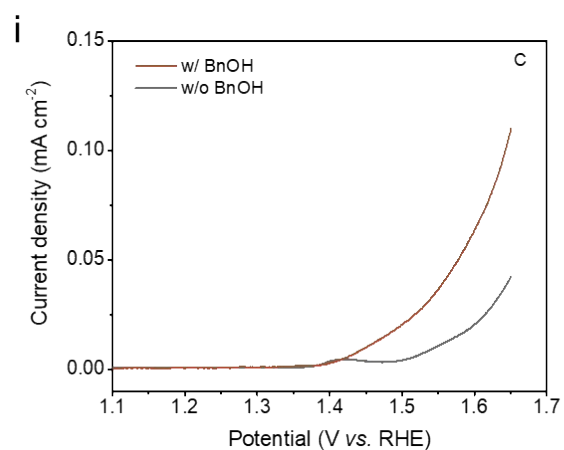


Figure S3 LSV curves of **a)** Mn plate, **b)** Co foam, **c)** Ni foam, **d)** Cu foam, **e)** Ru plate, **f)** Fe foam, **g)** Pd plate, **h)** Pt plate and **i)** carbon paper without (grey line) and with (brown line) BnOH at a scan rate of 5 mV/s with stirring (pH 13, without NH_3).

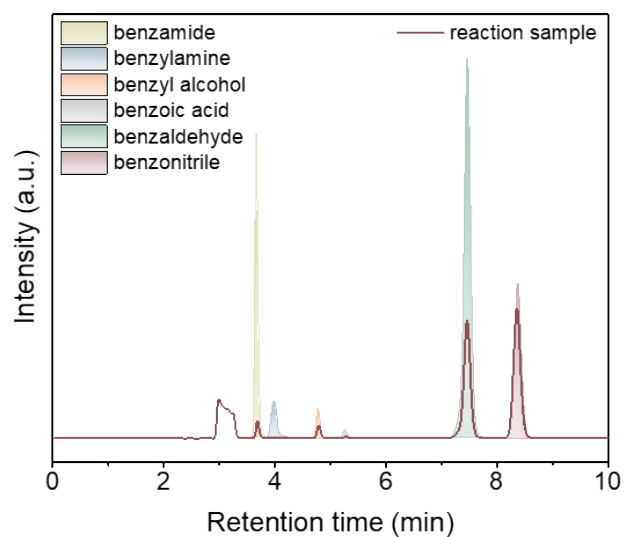


Figure S4 HPLC chromatograms of the standards (shaded peaks) and reaction sample (red line) at 269 nm UV absorption wavelength.

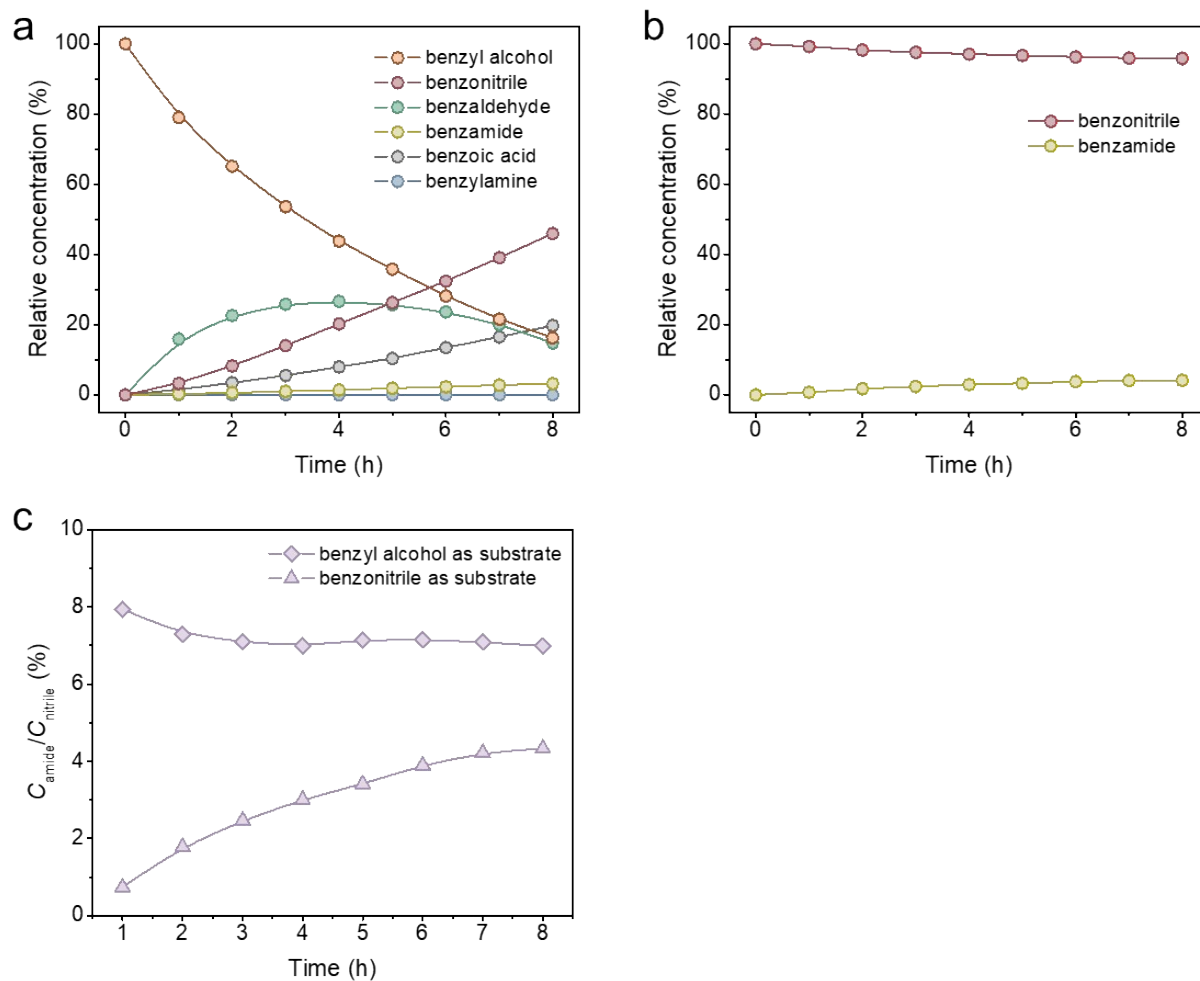


Figure S5 Relative concentrations of the reaction participants using **a)** benzyl alcohol and **b)** benzonitrile as the substrate. **c)** The ratio of concentrations of benzamide to benzonitrile during the reaction. Reaction conditions: Ni foam, 20 mM substrate, 1 M NH_3 , pH 13, 1.425 V vs. RHE.

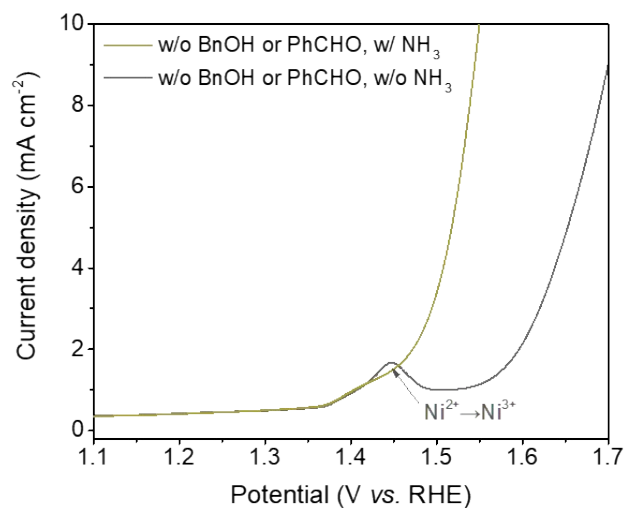
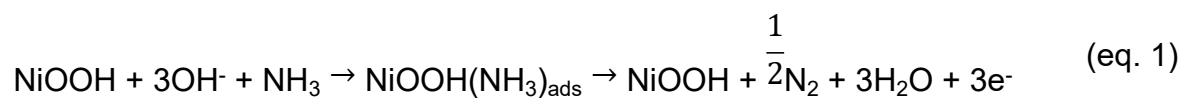


Figure S6 LSV curves of Ni foam without (grey line) and with (yellow line) NH_3 at a scan rate of 10 mV/s without stirring (pH 13).

The oxidative wave when ammonia is present corresponds to the direct oxidation of ammonia by NiOOH (eq. 1):¹



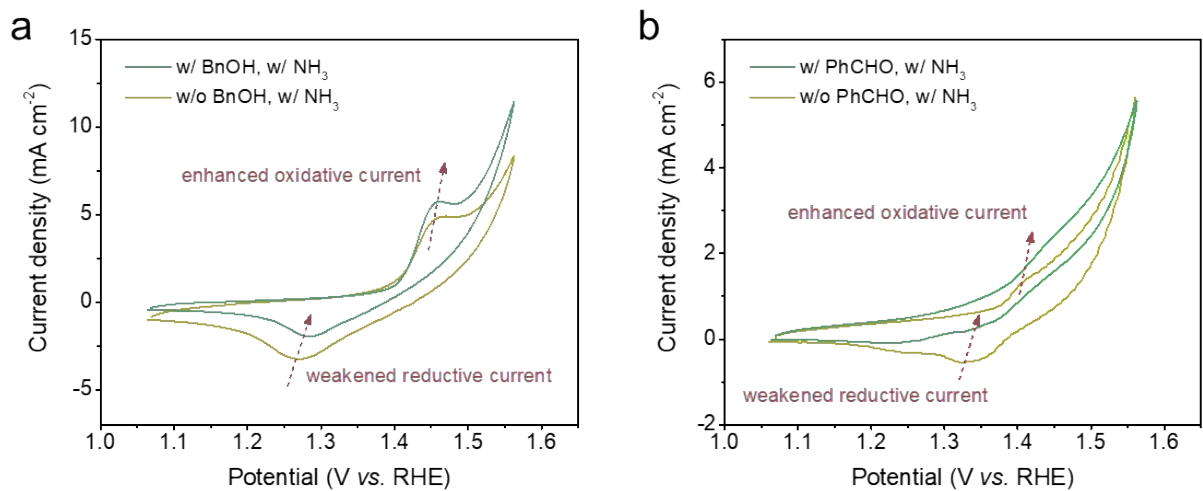


Figure S7 CV curves of Ni foam **a)** without (yellow line) and with (green line) BnOH, **b)** without (yellow line) and with (green line) PhCHO at a scan rate of 200 mV/s without stirring (with NH₃, pH 13).

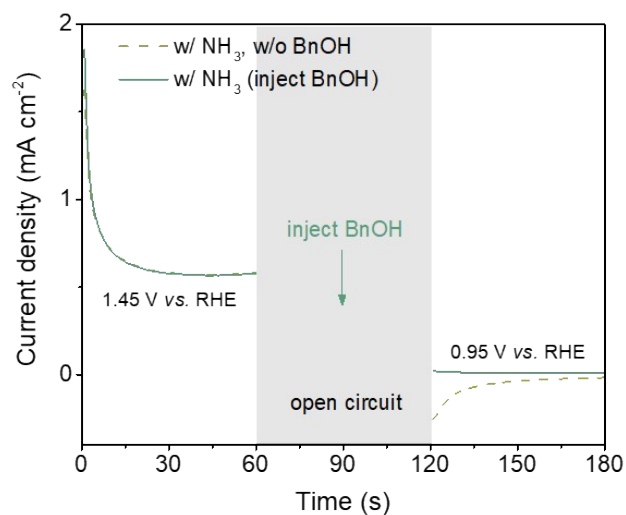


Figure S8 Multi-potential chronoamperometry test of Ni foam in 1 M NH_3 electrolyte solution (pH 13).

At a high potential of 1.45 V vs. RHE, the oxidative current is ascribed to the transformation of Ni^{2+} to Ni^{3+} . When the potential was changed to 0.95 V vs. RHE after the open circuit state, the current for the reduction of Ni^{3+} to Ni^{2+} was observed. Notably, the reduction current disappeared when BnOH was injected in the electrolyte solution during the open circuit state, indicating the reduction of Ni^{3+} to Ni^{2+} had taken place prior through extracting hydrogen atoms from BnOH.

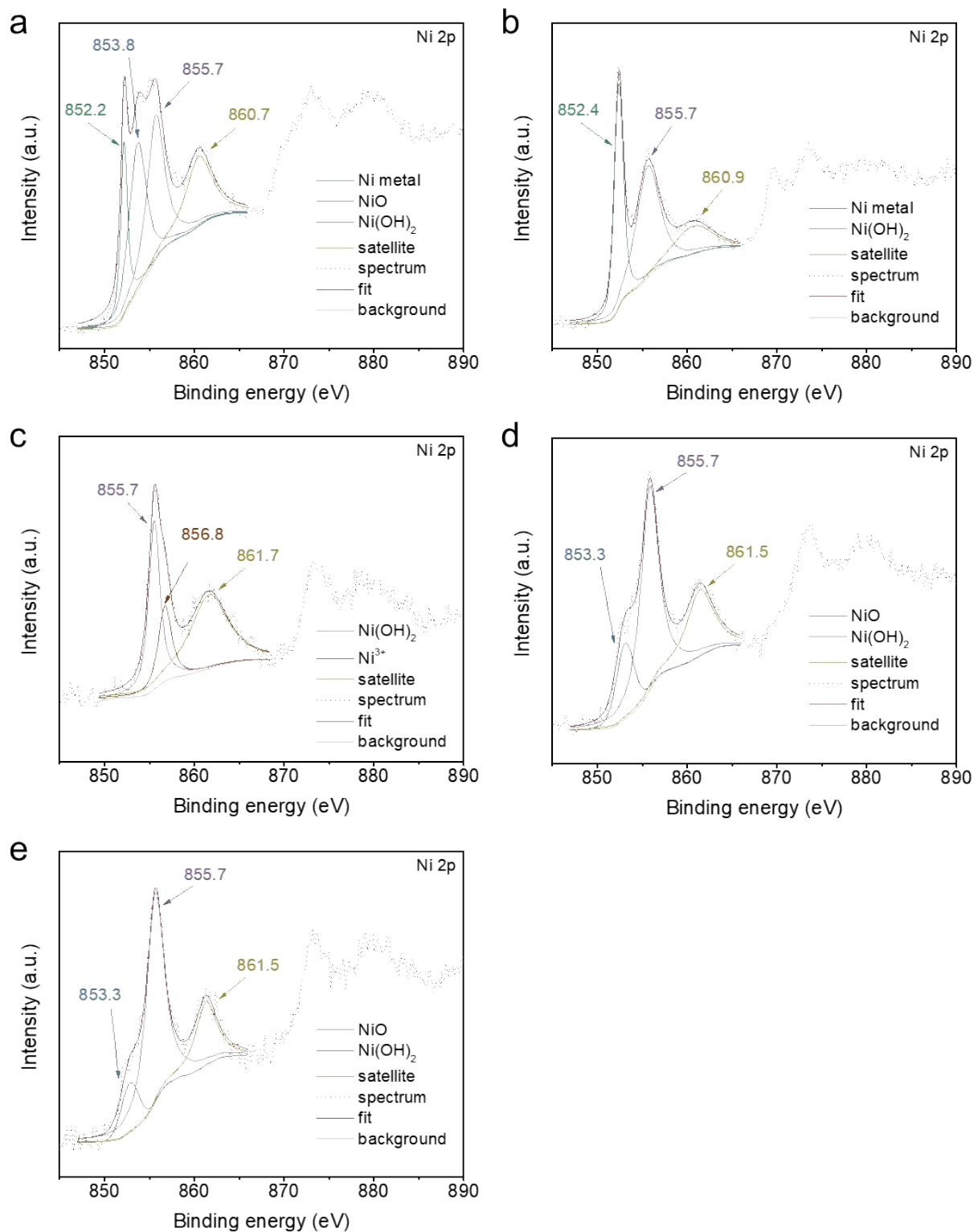


Figure S9 XPS high resolution Ni 2p spectra of Ni foam **a)** before HCl treatment, **b)** after HCl treatment, **c)** after applying 1.45 V vs. RHE, and after stirring the potential-treated Ni foam in an electrolyte solution containing **d)** BnOH and NH_3 , **e)** PhCHO and NH_3 .

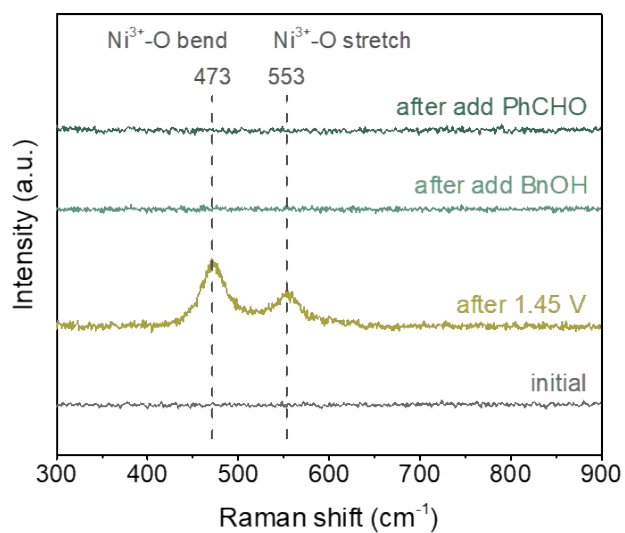


Figure S10 Raman spectra of Ni foam before applying potential (grey line), after applying 1.45 V vs. RHE (yellow line), and after stirring the potential-treated Ni foam in an electrolyte solution containing NH_3 and BnOH (light green line) or PhCHO (dark green line).

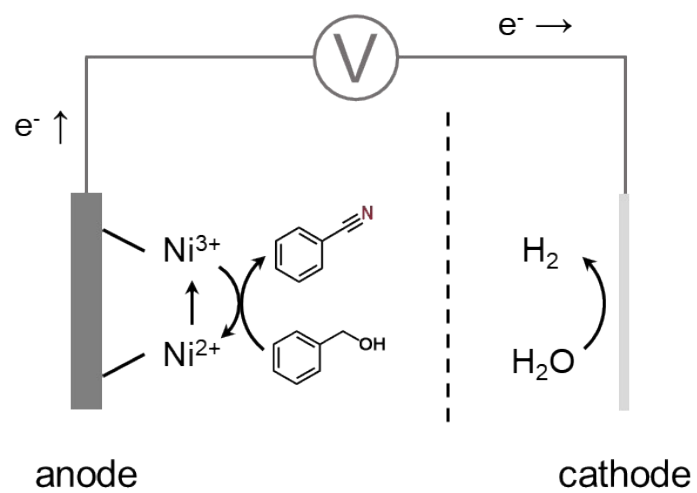


Figure S11 Schematic diagram of the proposed steps in the C-N coupling of benzyl alcohol and ammonia to benzonitrile on Ni foam.

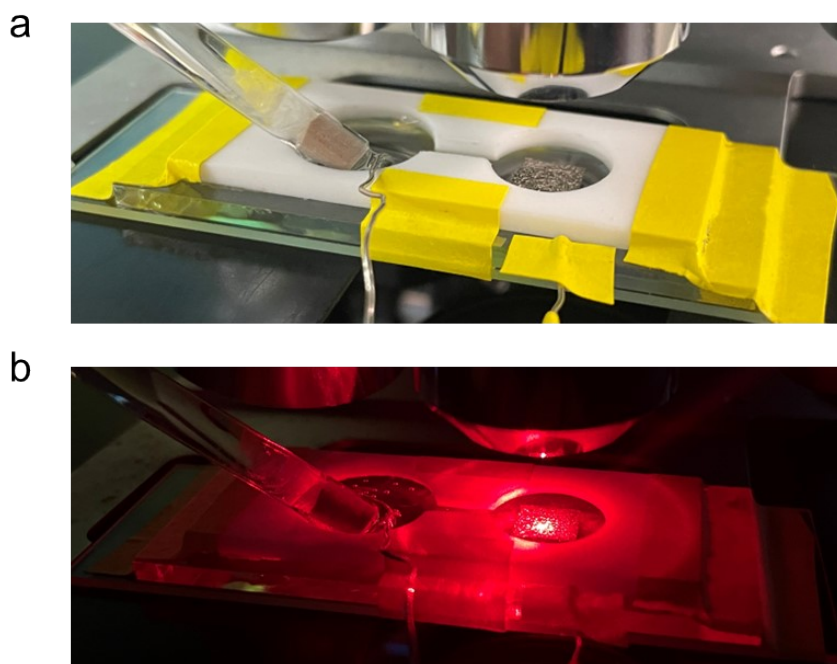


Figure S12 a) Homemade electrochemical cell for *in-situ* Raman studies. b) Snapshot of experimental setup during *in-situ* Raman investigation.

The *in-situ* Raman electrochemical cell consists of a Teflon body, with two compartments connected by a narrow channel. The Teflon body is secured to a fluorine-doped tin oxide (FTO) conductive glass base in a leak-proof manner. The working electrode is nickel foam that has been pre-treated using identical procedures to those before electrocatalytic reactions. The reference electrode is a Hg/HgO electrode while the counter electrode is a Pt wire electrode. The working electrode is stuck to the smaller compartment using conductive carbon double-sided tape, while the reference and counter electrodes are immersed in the larger compartment. The narrow channel acts to minimise the movement of gas bubbles produced at the counter electrode towards the working electrode and interference with Raman measurements.

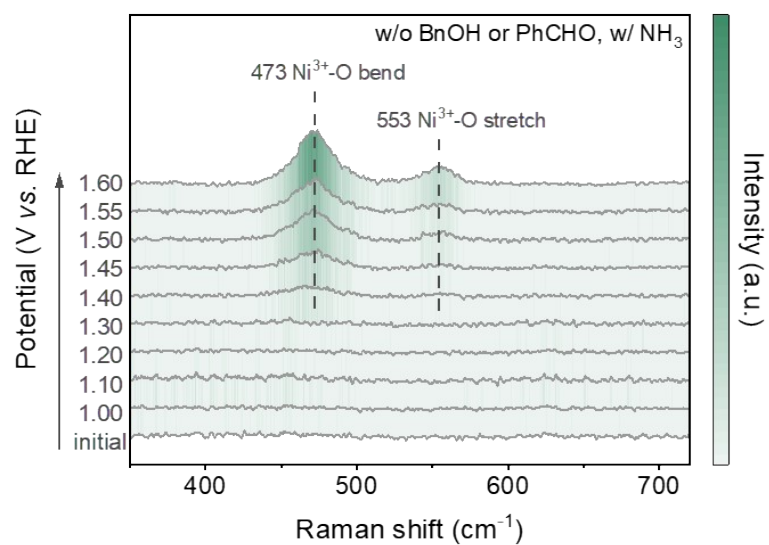


Figure S13 2D spectrum for the potential-dependent *in-situ* Raman studies of Ni foam in an electrolyte solution with NH₃.

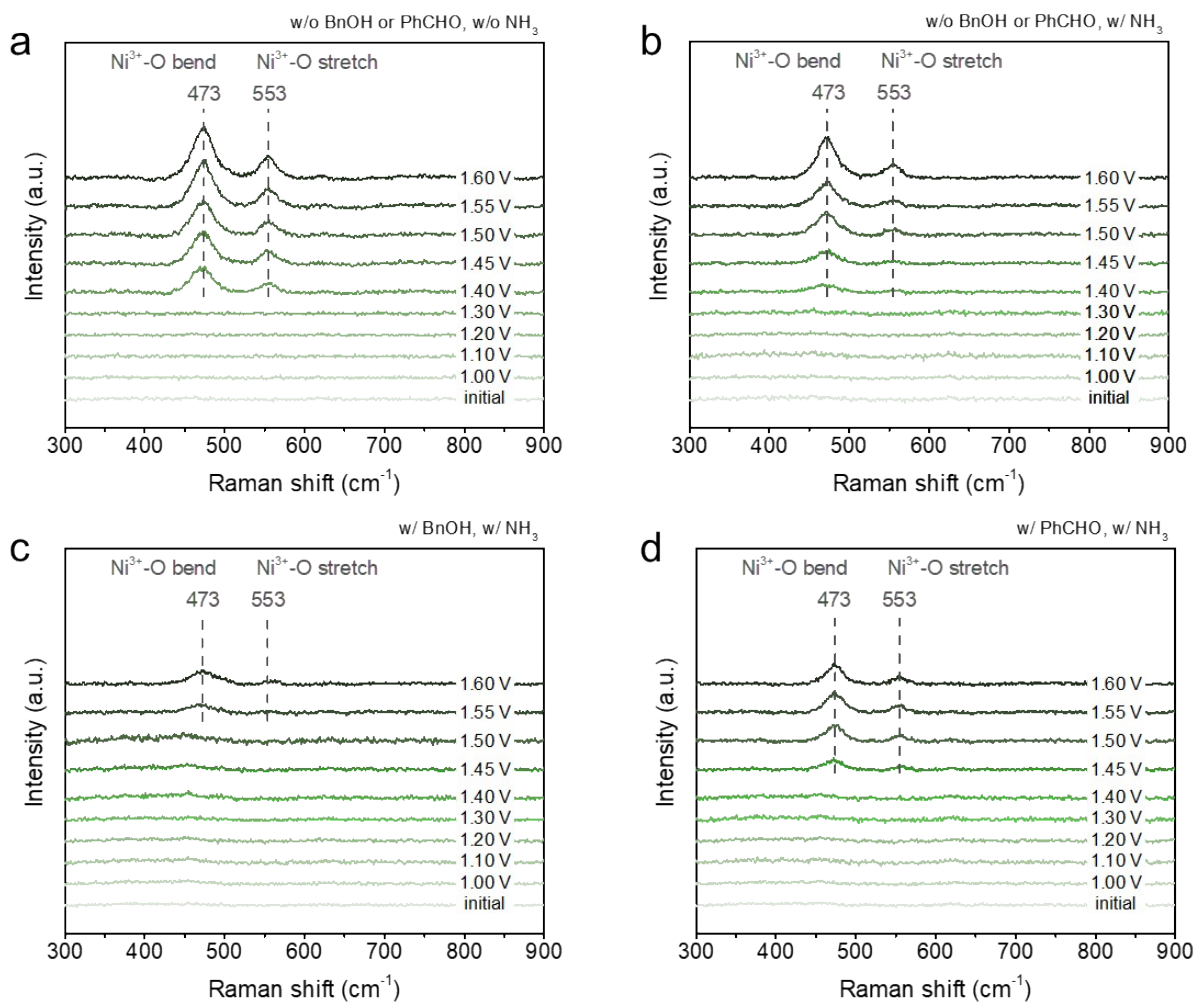


Figure S14 Potential-dependent *in-situ* Raman spectra of Ni foam **a)** without BnOH, PhCHO or NH_3 ; **b)** without BnOH or PhCHO, with NH_3 ; **c)** with BnOH and NH_3 ; **d)** with PhCHO and NH_3 .

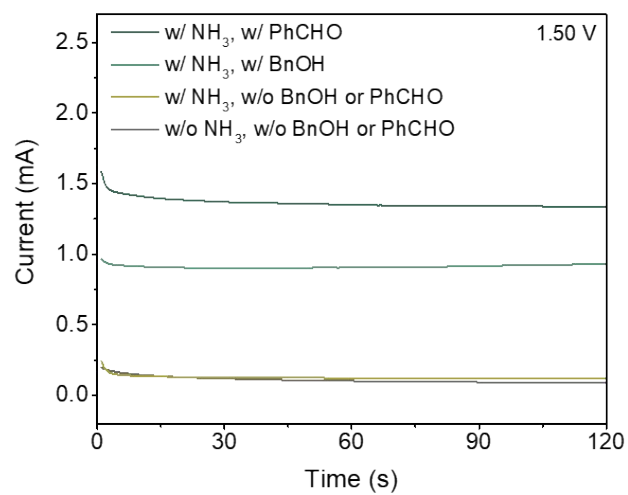


Figure S15 Currents recorded under the *in-situ* Raman measurements at 1.50 V vs. RHE.

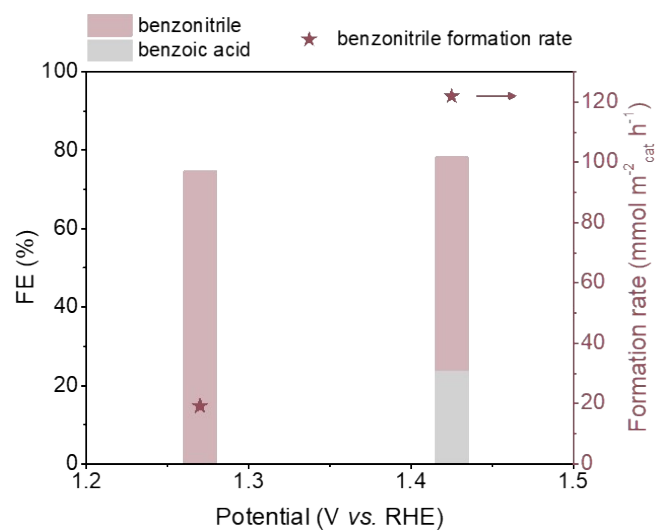


Figure S16 FEs and PhCN formation rate of the electro-oxidative coupling of PhCHO and NH₃ on Ni foam for 5 h under different applied potentials (20 mM PhCHO, 1 M NH₃, pH 13).

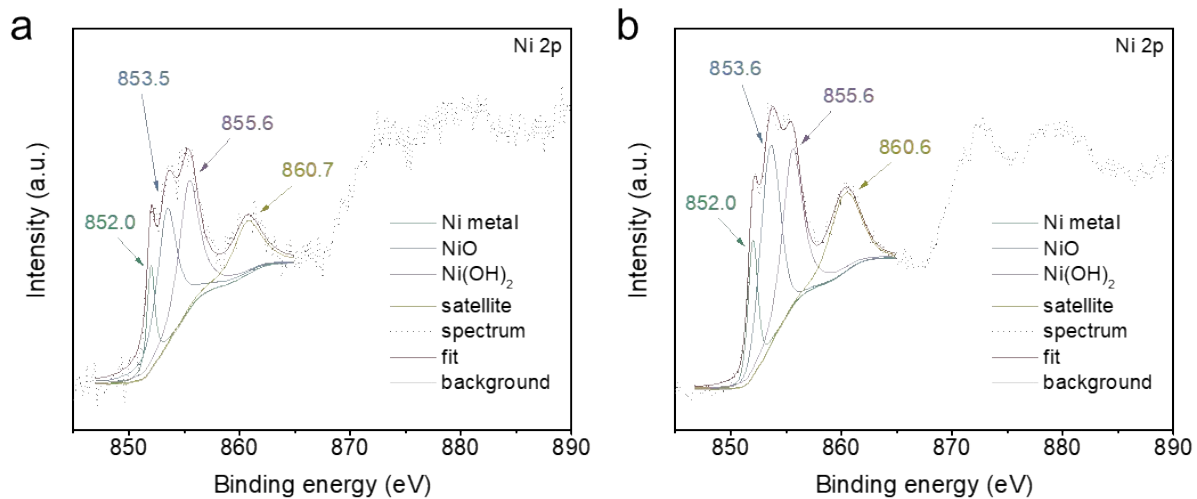


Figure S17 XPS high resolution Ni 2p spectra of Ni foam after applying 1.27 V vs. RHE **a**) with and **b**) without PhCHO and NH₃ in the electrolyte.

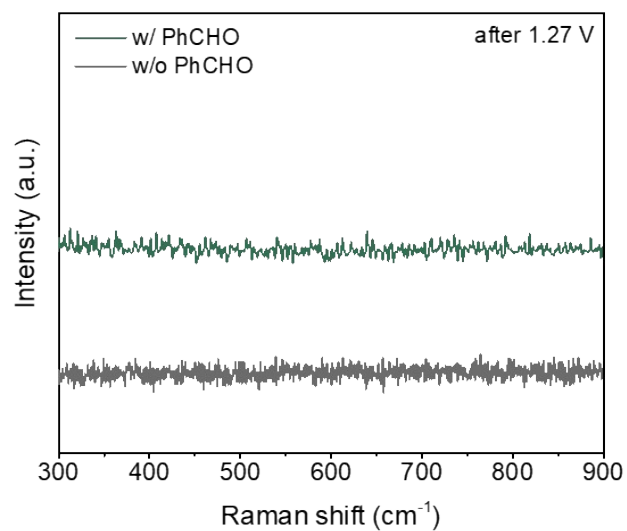


Figure S18 Raman spectra of Ni foam after applying a potential at 1.27 V vs. RHE without (grey line) and with (green line) PhCHO.

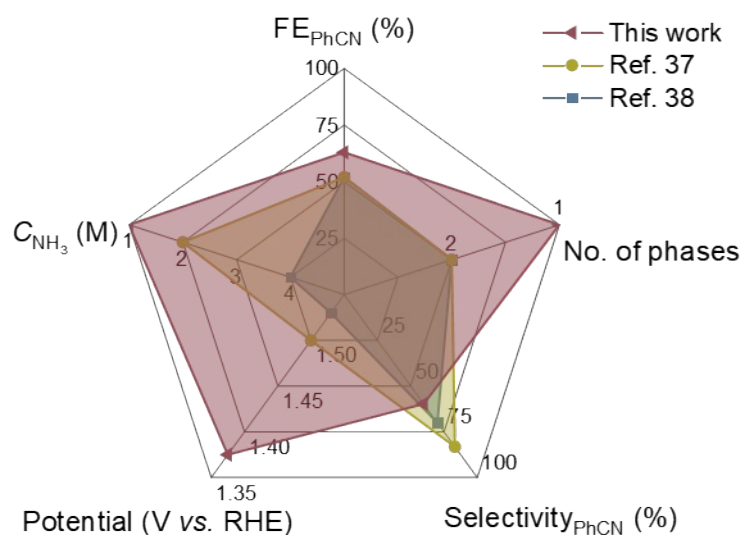


Figure S19 Comparison of PhCN FE (FE_{PhCN}) and selectivity ($Selectivity_{PhCN}$), applied potential, concentration of NH_3 (C_{NH_3}) and number of catalyst phases (No. of phases) over our Ni foam catalyst against reported catalysts. The reference numbers refer to those used in the main text.

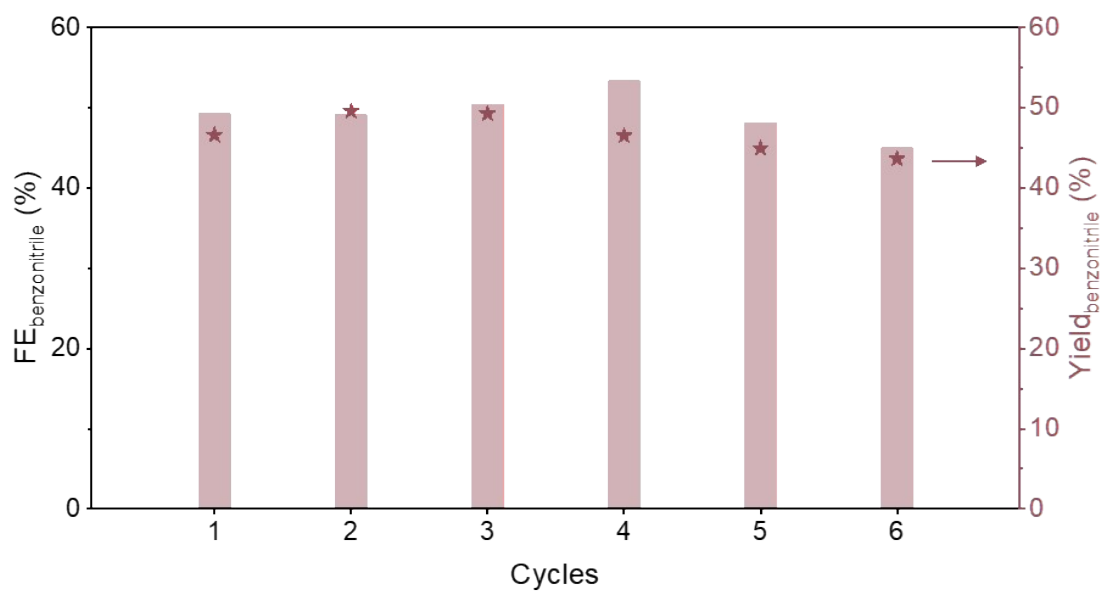


Figure S20 Recycling test of the electro-oxidative coupling of BnOH and NH₃ on Ni foam (20 mM BnOH, 1 M NH₃, pH 13, 1.425 V vs. RHE, 12 h).

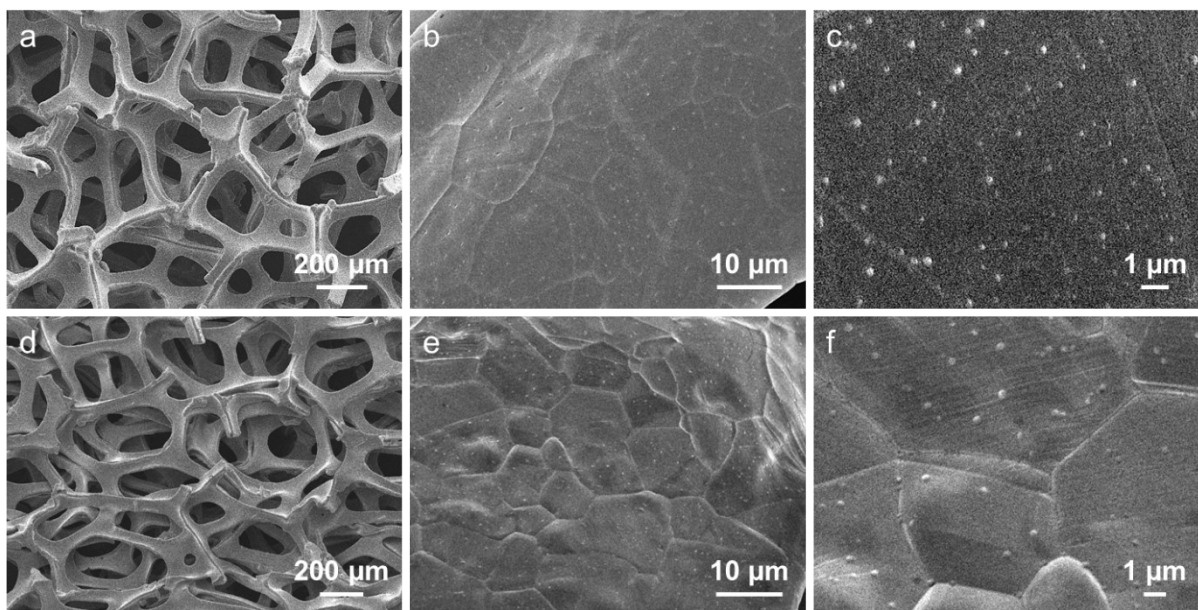


Figure S21 SEM images of the Ni foam before (a, b, c) and after (d, e, f) reaction (20 mM BnOH, 1 M NH₃, pH 13, 1.425 V vs. RHE, 12 h).

Both fresh and spent samples exhibit porous network structure with vein-like patterns, dents and protrusions on the rough surfaces.

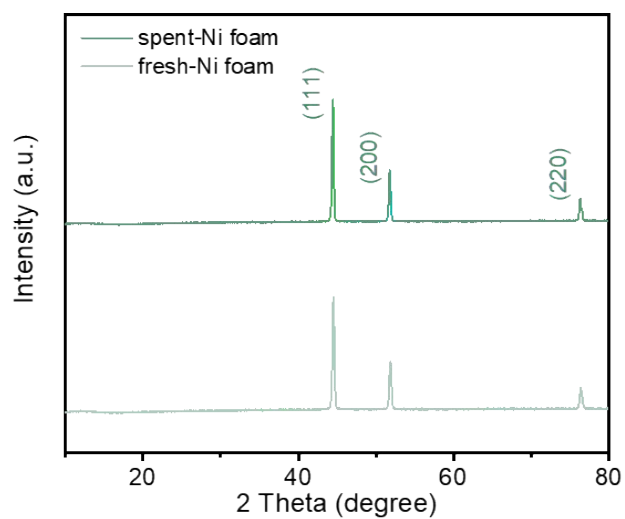


Figure S22 XRD patterns of the Ni foam before and after reaction (20 mM BnOH, 1 M NH_3 , pH 13, 1.425 V vs. RHE, 12 h).

The peaks at 44.5° , 51.9° and 76.4° are attributed to (111), (200) and (220) lattice planes of Ni (PDF #04-0850), respectively.

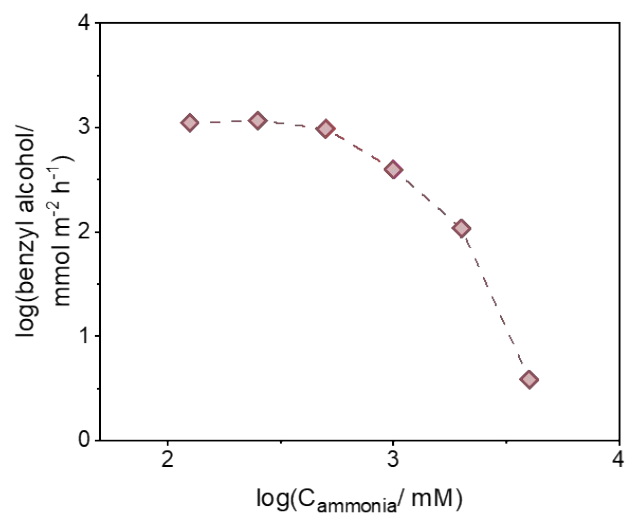


Figure S23 The dependence of BnOH consumption rate on the concentration of NH_3 (20 mM BnOH) at pH 13, 1.425 V vs. RHE and conversion around 20%.

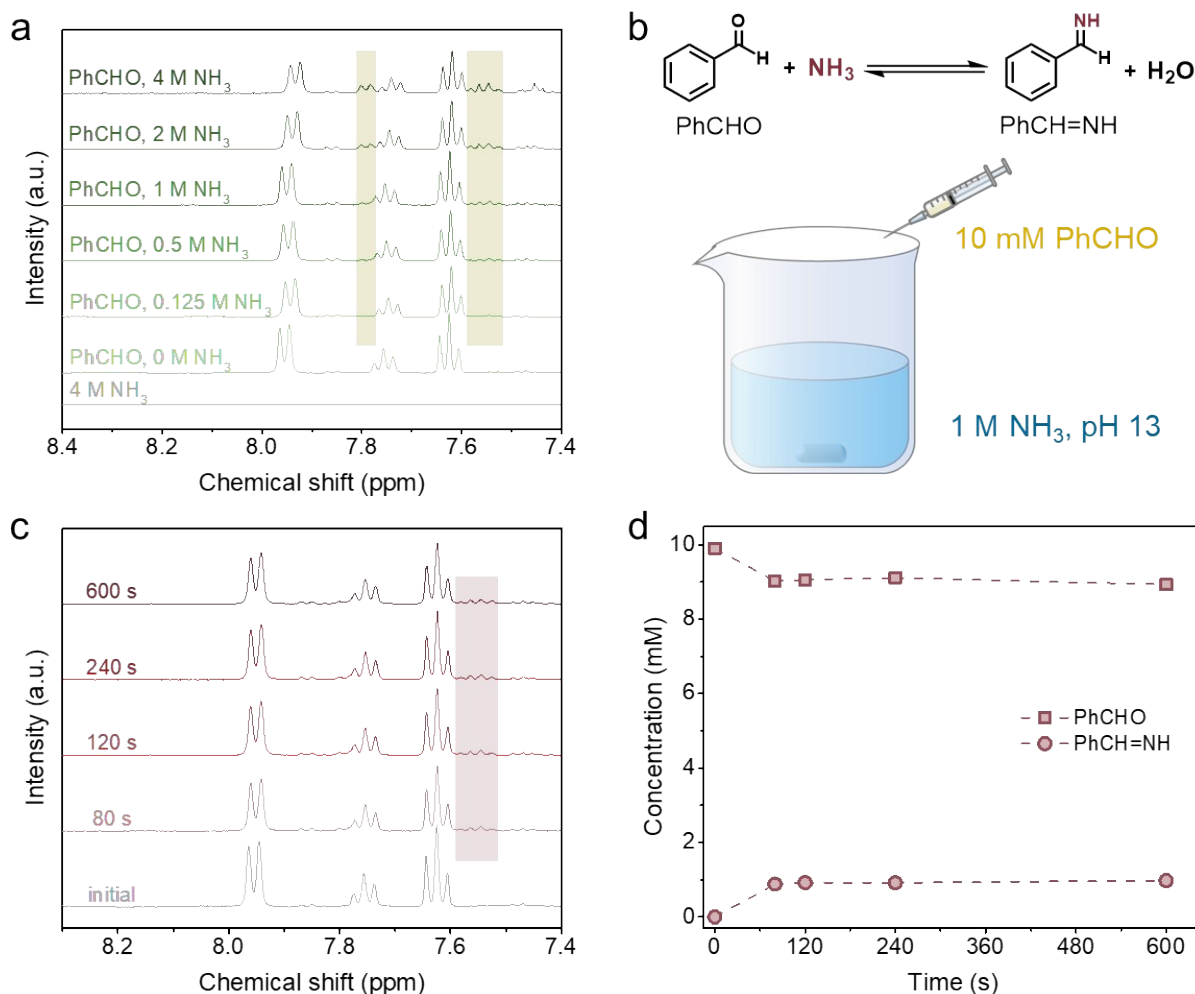


Figure S24 Identification and detection of the primary imine formed by the condensation between PhCHO and NH₃. **a)** ¹H NMR spectra of the electrolyte solutions containing 4 M NH₃ (grey line), as well as 10 mM PhCHO with different concentrations of NH₃ (0-4 M, green lines). **b)** Schematic illustration of the experiment for the formation of PhCH=NH. **c)** ¹H NMR spectra of the electrolyte solution obtained during the reaction. **d)** The amounts of PhCHO and PhCH=NH during the reaction. Reaction conditions: 10 mM PhCHO, 1 M NH₃, pH 13.

To identify the NMR peaks attributed to PhCH=NH, we prepared a series of electrolyte solutions containing 10 mM PhCHO with different concentrations of NH₃ and measured their NMR spectra (Fig. S24a). 4 M NH₃ electrolyte solution was also analysed. As the NH₃ concentration increased from 0 M to 4 M, two peaks located at ~7.56 ppm and ~7.79 ppm appeared and increased, which were not present in the solution containing only PhCHO or only NH₃. Thus, we assigned these peaks to PhCH=NH.

After confirming the peak position of PhCH=NH, we performed an experiment for the generation and detection of PhCH=NH (Fig. S24b). 41 μL of PhCHO (10 mM) was injected into 40 mL of 1 M NH_3 electrolyte solution (pH 13) under stirring, and the timing was started. When the solution was visually homogeneous ($t = 80$ s), we did the sampling immediately. The reaction solution was analysed using ^1H NMR throughout the entire period. As displayed in the NMR spectra (Fig. S24c) and concentration profile (Fig. S24d), the amount of PhCH=NH reaches its highest value (~ 0.925 mM) at 80 s and levels off, indicating that the equilibrium between PhCHO and PhCH=NH is achieved very rapidly (within 80 s).

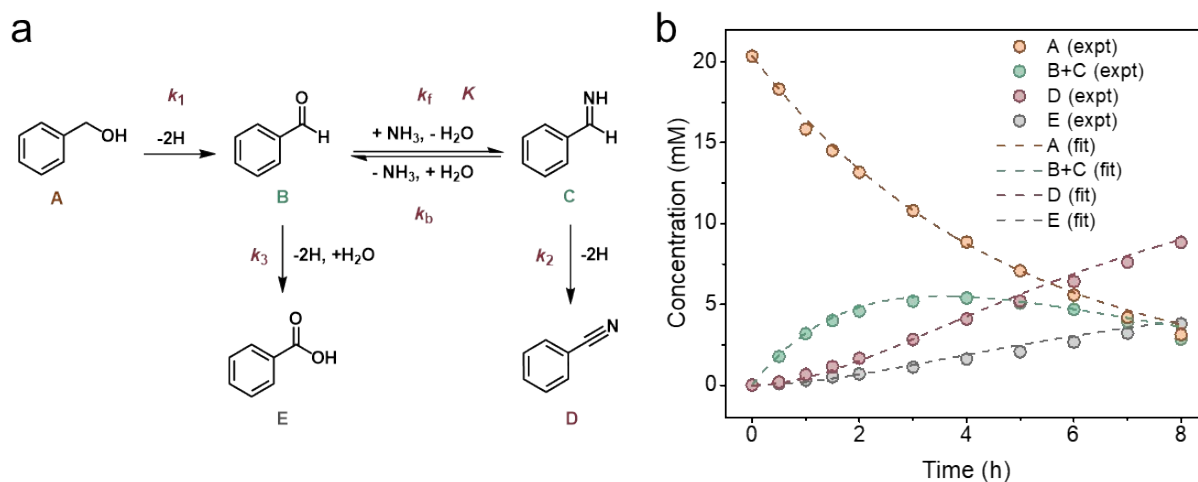


Figure S25 Kinetic modelling of the electro-synthesis of benzonitrile from benzyl alcohol and ammonia. a) Simplified reaction pathway used for modelling. b) Experimental results (circles) and model prediction (dashed line) for the concentration profiles of benzyl alcohol (A), benzaldehyde and corresponding imine (B+C), benzonitrile (D) and benzoic acid (E) during electrolysis.

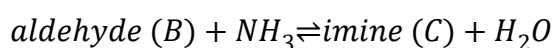
Using NMR spectroscopy, we quantify the concentrations of aldehyde (B) and imine (C) as a function of time. Both concentrations were found to attain steady values within 80 s of mixing (Fig. S24).

The equilibrium constant for the aldehyde (B)-imine (C) equilibrium (K) can be calculated:

$$K = \frac{[C]}{[B][NH_3]} = \frac{0.925 \text{ mM}}{9.03 \text{ mM} \times 1000 \text{ mM}} = 1.02 \times 10^{-4} \text{ mM}^{-1}$$

As ammonia is in large excess, we also estimate the minimum pseudo first-order rate

constant (k_f') for the reaction between aldehyde (B) and ammonia to form imine (C):



$$\text{Rate} = k_f[B][NH_3] \approx k_f'[B]$$

$$\frac{0.925 \text{ mM}}{80 \text{ s}} = k_f' \times \frac{9.90 \text{ mM} + 9.03 \text{ mM}}{2}$$

$$k_f' = 1.22 \times 10^{-3} \text{ s}^{-1} = 4.40 \text{ h}^{-1}$$

The aldehyde (B)-imine (C) equilibrium is always achieved instantaneously, as verified earlier:

$$K = \frac{k_f}{k_b} = \frac{[C]}{[B][NH_3]} \Rightarrow [C] = K[NH_3][B]$$

Since the product quantification gave the combined concentration of the aldehyde (B) and imine (C), we express the individual concentrations [B] and [C] in terms of ([B] + [C]):

$$\frac{[B]}{[B] + [C]} = \frac{[B]}{[B] + K[NH_3][B]} = \frac{1}{1 + K[NH_3]} \Rightarrow [B] = \frac{[B] + [C]}{1 + K[NH_3]}$$

$$\frac{[C]}{[B] + [C]} = \frac{K[NH_3][B]}{[B] + K[NH_3][B]} = \frac{K[NH_3]}{1 + K[NH_3]} \Rightarrow [C] = \frac{K[NH_3]([B] + [C])}{1 + K[NH_3]}$$

The rate equations can now be written for [A], ([B] + [C]), [D] and [E]:

$$\frac{d[A]}{dt} = -k_1[A]$$

$$\frac{d([B] + [C])}{dt} = k_1[A] - k_2 \frac{K[NH_3]([B] + [C])}{1 + K[NH_3]} - k_3 \frac{[B] + [C]}{1 + K[NH_3]}$$

$$\frac{d[D]}{dt} = k_2 \frac{K[NH_3]([B] + [C])}{1 + K[NH_3]}$$

$$\frac{d[E]}{dt} = k_3 \frac{[B] + [C]}{1 + K[NH_3]}$$

By using the least-squares function for non-linear systems (`lsqnonlin`) and a suitable solver for ordinary differential equations (`ode45`) in MATLAB, the above set

of simultaneous ODEs were numerically solved and the optimised parameters were obtained, where we have used the earlier obtained value of $K = 1.02 \times 10^{-4} \text{ mM}^{-1}$:

$$k_1 = 0.211 \pm 0.006 \text{ h}^{-1}$$

$$k_2 = 2.77 \pm 0.14 \text{ h}^{-1}$$

$$k_3 = 0.13 \pm 0.01 \text{ h}^{-1}$$

As shown in Fig. S25b, the kinetic model prediction agrees reasonably well with the experimental results, indicating that the model is suitable for describing the reaction scheme. We note that the earlier obtained value of $k_f' = 4.40 \text{ h}^{-1}$ is at least 59% larger than any of the above rate constants, which is consistent with our assumption that the aldehyde-imine equilibrium is established rapidly.

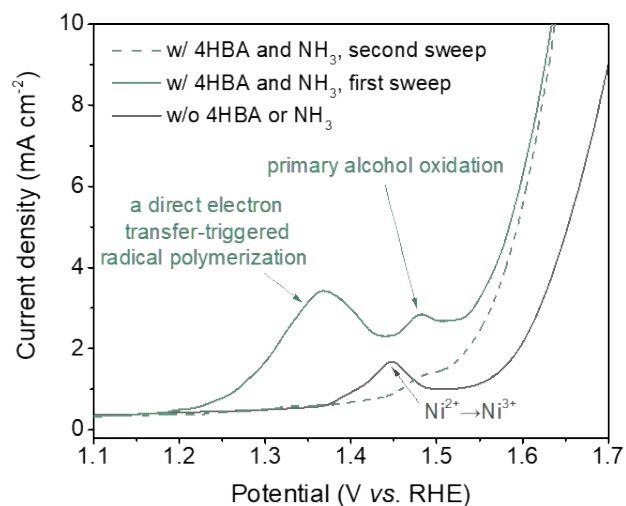


Figure S26 LSV curves of Ni foam without (grey line) and with (green line) 4-hydroxybenzyl alcohol (4HBA) and NH_3 at a scan rate of 10 mV/s without stirring (pH 13). The solid and dashed green lines correspond to the first and second sweeps, respectively.

As indicated by the solid green line in Fig. S26, there are two oxidation peaks during the first sweep in the presence of 4HBA. The first peak is attributed to a direct electron transfer to the phenoxide ion leading to the radical polymerization of 4HBA, which may cause rapid and strong passivation of Ni.^{2,3} This is also reflected in the second sweep (dashed green line) displaying that the first oxidation peak disappears and the second peak, which is ascribed to the oxidation of the primary alcohol, is weakened.

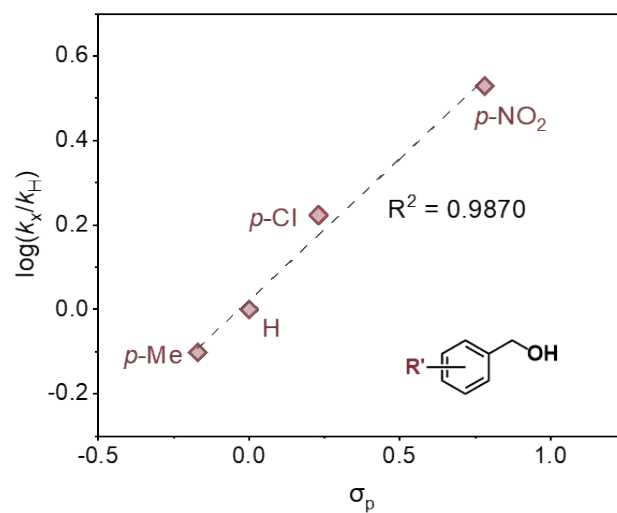


Figure S27 Hammett plot of Ni foam-catalysed electro-oxidative coupling of primary alcohols and ammonia. Reaction conditions: 5 mM primary alcohol, 1 M NH₃, pH 13, 1.425 V vs. RHE, around 20% conversion.

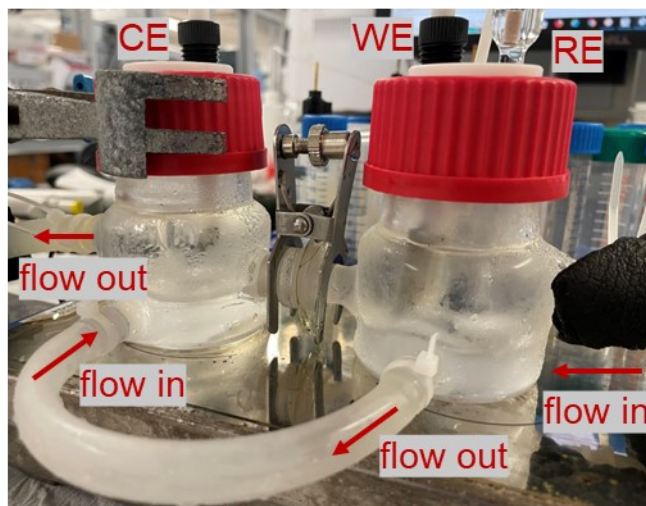


Figure S28 Experimental setup for the temperature-controlled electrosynthesis of PhCN.

In these tests, we used a jacketed electrochemical H-cell to control the reaction temperature, where water of the appropriate temperature was flowed through the external jacket, and allowed sufficient time for the temperature of the electrolyte solutions to stabilise before starting the potentiostatic experiments.

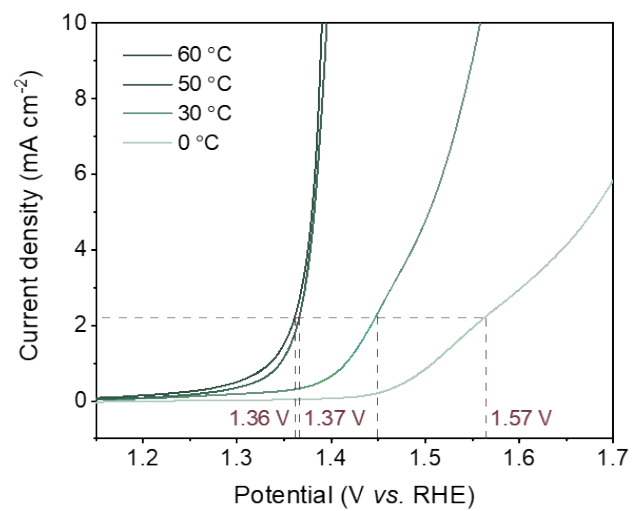
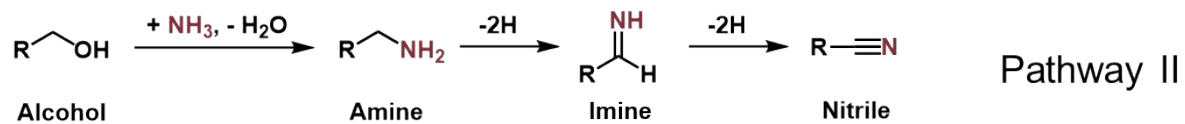
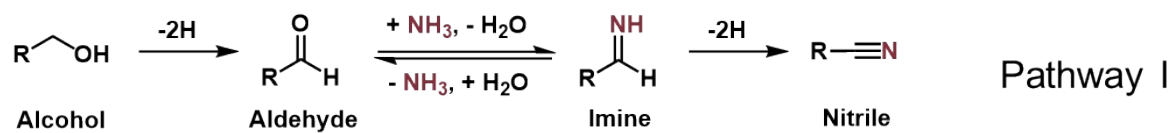
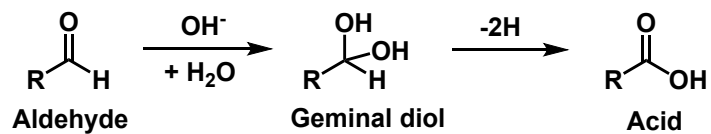
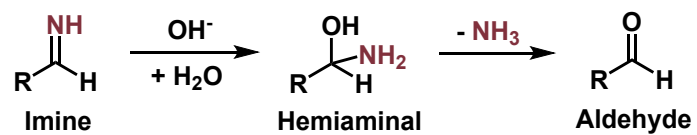


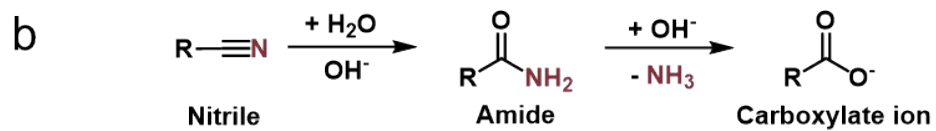
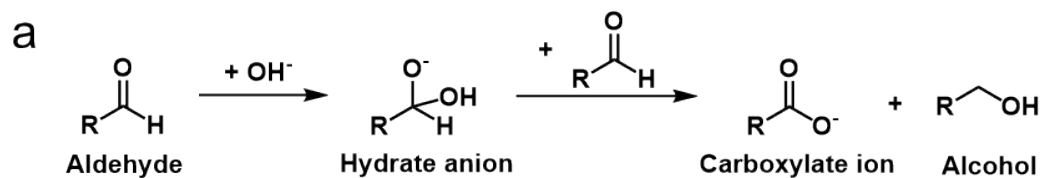
Figure S29 LSV curves of Ni foam at different temperatures with BnOH and NH₃ at a scan rate of 10 mV/s without stirring (pH 13).



Scheme S1 Two possible reaction pathways for the nitrile synthesis from primary alcohols and ammonia.



Scheme S2 Possible reasons for the high selectivity towards acid at high pH. OH⁻-catalysed hydrations of imine and aldehyde are beneficial for the acid formation.



Scheme S3 Simplified reaction schemes for **a)** Cannizzaro reaction and **b)** OH⁻-catalysed nitrile hydrolysis reaction.

Table S1 Existing works on the thermal catalytic synthesis of nitrile from alcohol.

Ref .	Temperature (°C)	Pressure (bar)	Duration (h)	Catalyst	Oxidant
22	120	10	24	graphitic-shell-encapsulated cobalt nanoparticles	O ₂
23	100	20	5	Ru/MnO ₂	O ₂
24	120	6	5	Ru(OH) _x /Al ₂ O ₃	O ₂
25	55	1	24	CuI (bpy, TEMPO)	O ₂
26	130	5	18	Co-phenanthroline/C, Fe-phenanthroline/C	O ₂
27	130	5	18	Co-N/C	O ₂
28	various, mostly >50	various, mostly >5	various	various	various
29	280	1	N.A. (flow reactor)	Cu/m-ZrO ₂	-
30	190	1	N.A. (flow reactor)	Ni/Al ₂ O ₃	-
31	160	1	N.A. (flow reactor)	Ni _{0.5} Cu _{0.5} /Al ₂ O ₃	-

Table S2 Electrocatalytic performance of selected materials on the synthesis of PhCN under higher oxidative potentials.

Material s	Potential (V vs. RHE)	Conversion (%)	PhCN yield (%)	PhCN FE (%)
Fe	1.650	27.3	3.19	3.13
Pd	2.025	4.19	0.032	0.020
Pt	2.225	7.55	0.19	0.71
C	2.025	9.17	0.49	1.6

Reaction conditions: 20 mM BnOH, 1 M NH₃, pH 13, 8 h reaction time.

In Figure 2, we performed electrolysis at 1.425 V vs. RHE where Fe, Pd, Pt and C exhibit no significant current at this potential as shown in their LSV curves. We suspected that 1.425 V may not be high enough for the electrosynthesis of PhCN on these materials. Thus, we conducted further experiments using more oxidative applied potentials but there was still only negligible PhCN product. During potentiostatic experiments at potentials above 1.425 V, although there was detectable current on all four of the materials, the FE towards PhCN was very low (below 3%, comparable to experimental uncertainties in certain cases), implying that the majority of the current was attributed to processes other than the transformation of organic compounds, such as electrode oxidation, NH₃ oxidation and oxygen evolution reaction (OER).

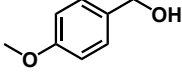
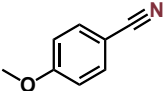
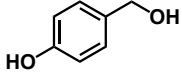
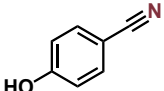
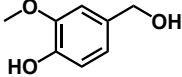
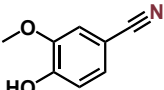
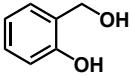
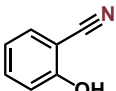
Table S3 ICP-OES quantification of Ni element in the electrolyte before and after reaction.

	Before	After	Change
Ni (ppm)	0.920	3.443	2.523

Reaction conditions: Ni foam, 20 mM BnOH, 1 M NH₃, pH 13, 1.425 V vs. RHE, 12 h reaction time.

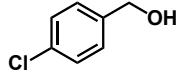
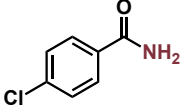
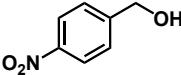
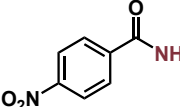
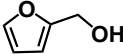
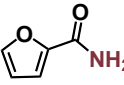
The Ni content in the electrolyte after 12 h reaction was 2.523 ppm (4.299×10^{-5} mol/L). Since the electrolyte volume was 40 mL, the amount of Ni was calculated to be 1.720×10^{-6} mol. The weight of the Ni foam used for the reaction was 0.1646 g, which contained 2.805×10^{-3} mol Ni assuming it was composed of only metallic Ni. Based on the above calculations, we could conclude that the extent of Ni leaching was very small, with only less than 1‰ (by mass) of the Ni foam dissolved.

Table S4 Electrosynthesis of nitriles using aromatic substrates with electron-donating groups.

	Substrate	Product	Conversion/Selectivity (%)
j			4-methoxybenzyl nitrile 39.6/19.2
k			4-hydroxybenzyl nitrile 0.87/1.6
l			4-hydroxy-3-methoxybenzyl nitrile 0.20/-
m			2-hydroxybenzyl nitrile 0.93/2.0

Reaction conditions: Ni foam, 20 mM primary alcohol, 1 M NH₃, pH 13, 1.425 V vs. RHE, 8 h reaction time.

Table S5 Conversions for the electro-oxidative coupling of primary alcohols and ammonia and selectivities for corresponding amides.

	Substrate	Product	Conversion/Selectivity (%)
c			4-chlorobenzamide 87.8/18.0
d			4-nitrobenzamide 99.3/24.3
ja			2-furamide 47.9/50.9

Reaction conditions: Ni foam, 5 mM primary alcohol (^a 20 mM), 1 M NH₃, pH 13, 1.425 V vs. RHE, 8 h reaction time.

Table S6 Existing works and our approach for the electrocatalytic synthesis of nitrile from alcohol.

Ref.	Temperature (°C)	C _{ammonia} (M)	Potential (V vs. RHE)	Duration (h)	Catalyst	PhCN Yield (%)	PhCN FE (%)
Our work	50	1	1.392	5	Ni foam	61.1	49.7
Our work	50	1	1.379	6	Ni foam	59.9	52.9
Our work	50	1	1.376	6	Ni foam	55.8	55.7
Our work	50	1	1.367	8	Ni foam	54.1	61.6
37	room	2	1.50	4	Pd/CuO	83.2	~50
38	room	4	1.53	12	NiCo-N,O/CC	74	52

References

1. A. Kapałka, A. Cally, S. Neodo, C. Comninellis, M. Wächter and K. M. Udert, *Electrochem. Commun.*, 2010, **12**, 18-21.
2. P. Parpot, A. P. Bettencourt, A. M. Carvalho and E. M. Belgsir, *J. Appl. Electrochem.*, 2000, **30**, 727-731.
3. C. Z. Smith, J. H. P. Utley and J. K. Hammond, *J. Appl. Electrochem.*, 2011, **41**, 363-375.